ELSEVIER

Biophysical Chemistry 74 (1998) 237–249

Biophysical Chemistry

Intermembrane distance in multilamellar vesicles of phosphatidylcholine depends on the interaction free energy between solvents and the hydrophilic segments of the membrane surface

Kouji Kinoshita[a], Shou Furuike[b], Masahito Yamazaki[a,b,*]

[a] *Materials Science, Graduate School of Science and Engineering, Shizuoka University, Shizuoka, 422 Japan*
[b] *Department of Physics, Faculty of Science, Shizuoka University, 836 Oya, Shizuoka, 422 Japan*

Received 16 December 1997; accepted 13 July 1998

Abstract

To investigate the interaction of the surface of biomembranes with solvents systematically, we have studied the structure and phase behavior of multilamellar vesicles of dipalmitoylphosphatidylcholine (DPPC) and 1-palmitoyl-2-oleoyl-phosphatidylcholine (POPC) in dimethylformamide (DMF)–water mixture by X-ray diffraction and differential scanning calorimetry. The solubility of phosphorylcholine, which is the same molecular structure as the head-group of phosphatidylcholine (PC), decreased with an increase in DMF concentration. This result indicates that DMF is a poor solvent for the hydrophilic segments of the surface of the PC membrane, and interaction free energy of the hydrophilic segments of the membrane surface with solvents increases with an increase in DMF concentration. X-ray diffraction data indicated that DPPC-MLVs were in the bilayer gel phase from 0 to 80% (v/v) DMF, and that the spacing (lamellar repeat period) and intermembrane distance of DPPC-MLV decreased with an increase in DMF concentration. Main transition temperature and pre-transition temperature of DPPC-MLV increased with an increase in DMF concentration, and above 50% (v/v) DMF there was no pre-transition. In the interaction of POPC-MLV with DMF, X-ray diffraction data indicated that POPC-MLVs were in L_α phase (liquid-crystalline phase) from 0 to 80% (v/v) DMF, and that the spacing and intermembrane distance of POPC-MLV decreased with an increase in DMF concentration. These results are discussed by the change of the interaction free energy between the hydrophilic segments of the membrane surface and solvents. As DMF concentration increases, this interaction free energy may increase, resulting in the decrease of the intermembrane distance of PC-MLVs.

Keywords: χ parameter; Poor solvent; Gel phase; Phospholipid; Intermembrane distance; Undulation motion

* Corresponding author. Tel.: +81 54 2384741; e-mail: m-yamazaki@sci.shizuoka.ac.jp

Abbreviations: DPPC, 1,2-dipalmitoyl-*sn*-glycero-3-phosphatidylcholine; POPC, 1-palmitoyl-2-oleoyl-*sn*-glycero-3-phosphatidylcholine; MLV, multilamellar vesicle; L_α phase, liquid-crystalline phase; $L_{\beta'}$ phase, bilayer gel phase with tilted hydrocarbon chains; SAXS, small-angle X-ray scattering; WAXS, wide-angle X-ray scattering

0301-4622/98/$19.00
PII S0301-4622(98)00191-4

1. Introduction

Recently, the phospholipid–water interface in biomembranes has attracted much attention because it plays important roles in stability of phospholipid vesicles [1–6] and interactions of biomembranes with various kinds of solutes [7–15]. Conformations of head-groups of phospholipid at various hydration conditions have been determined by several physical methods, such as solid-state nuclear magnetic resonance (e.g. Ulrich and Watts [6]). Theoretical studies and molecular dynamics simulations of phospholipid membrane–water interfaces have been recently developed [16–20]. However, physical characterization of this phospholipid–water interface or surface of biomembranes is still insufficient, and roles of hydration and water structure in biomembranes are controversial [1].

On the other hand, in the field of polymer science, interaction of segments of polymers with solvents has an important role in structures and interactions of polymers in solution [21–23]. For example, polymers expand in good solvents which interact with the polymer segments favorably, while polymers shrink in poor solvents where the interaction free energy with polymer chains are large. This interaction is very important in the state of gels where polymer molecules reveal networks. Recently, Tanaka and his colleagues found phase transitions in equilibrium volume of ionic gels composed of acrylamide and acrylic acid [24–27]. Collapse of these gels in acetone–water mixtures occurred when the acetone concentration was increased or when the temperature was lowered. In these gels, acetone was a poor solvent. These phenomena were reasonably explained by the χ parameter (interaction free energy parameter) of polymer molecules and solvents.

In our previous paper [28], as our first investigation of effects of the interaction between a poor solvent and surface segments of biomembranes on structures and phase behaviors of the biomembrane, we studied the structure and phase behavior of multilamellar vesicles of dipalmitoylphosphatidylcholine (DPPC) in an acetone–water mixture by X-ray diffraction and differential scanning calorimetry. We found that acetone was a poor solvent of a hydrophilic segment of the head-group of phosphatidylcholine (PC) and that, as the acetone concentration increased, an interaction free energy, that is, a χ parameter, between the hydrophilic segments of the surface of DPPC membrane and solvents increased, resulting in the decrease of the solvent content inside the DPPC-MLV. However, acetone induced an interdigitated gel phase in DPPC-MLV at medium concentrations because acetone is a good solvent for the hydrophobic segments of the alkyl chains of the phospholipid, and also it is so small that it can penetrate into the interfacial regions of the phospholipid membranes [29]. Therefore the interpretation of the results became slightly complicated; we have to consider two effects, that is, effects of the poor solvent for the hydrophilic segments of the head-group and also the good solvent for the hydrophobic segments of the alkyl chains of the phospholipid membrane.

In this report, we have found that another water-soluble organic solvent, dimethylformamide (DMF), was a poor solvent for hydrophilic segments of the PC membrane and could not induce an interdigitated gel phase in DPPC-MLV. By using DMF, we have investigated effects of the poor solvent on structures and phase behaviors of DPPC-MLV in the $L_{\beta'}$ phase and POPC-MLV in the L_{α} phase. This research was presented at the 51th Annual Meeting of the Physical Society of Japan, March 1996 [31] and also at the 34th Annual Meeting of the Biophysical Society of Japan, November 1996 [32].

2. Materials and methods

2.1. Materials

1,2-Dipalmitoyl-*sn*-glycero-3-phosphatidylcholine (DPPC), and 1-palmitoyl-2-oleoyl-*sn*-glycero-3-phosphatidylcholine (POPC) were purchased from Avanti Polar Lipids Inc. Phosphorylcholine (chloride calcium salt) were purchased from Sigma Chemical Co. DMF (dimethylformamide) was purchased from Wako Chemical Co.

2.2. Sample preparation

Multilamellar vesicles (MLVs) were prepared by adding the appropriate amounts of DMF–water mixture of various concentrations of DMF to the dry lipids in excess solvents (~7 wt.% lipid), and the suspension was vortexed for approx. 30 s several times around 50°C for DPPC-MLV and at RT (~20°C) for POPC-MLV. MLV-suspensions at high concentrations of DMF were sonicated in a bath type sonicator for 15 s and three times after the above procedure. For measurement of X-ray diffraction, pellets (~50 wt.% lipid) after centrifugation ($14\,000 \times g$, 1 h at 20°C, Tomy, MR-150) of the suspensions were used.

2.3. X-ray diffraction

X-ray diffraction experiments were performed by using Nickel filtered Cu K_α X-radiation ($\lambda =$ 0.154 nm) from rotating an anode type X-ray generator (Rigaku, Rotaflex, RU-300, 50 kV, 300 mA). Small-angle X-ray diffraction (SAXS) data were recorded using a linear (one-dimensional) position sensitive proportional counter (PSPC) (Rigaku, PSPC-5) [33] with the sample-to-detector distance of 350 mm, and associated electronics (multichannel analyzer, etc., Rigaku). Wide-angle X-ray diffraction (WAXS) patterns were recorded by using PSPC with the sample-to-detector distance of 250 mm, and diffraction spacing was calibrated by using polyethylene [34]. In all cases, samples were sealed in a thin-walled glass capillary tube (outer diameter 1.0 mm) and mounted in a thermostatable holder whose stability was ±0.2°C [3].

SAXS data were processed by standard methods [28,33]. Integrated intensities of the various diffraction peaks, $I(h)$, where h is the order number, were determined after background subtraction. Measured intensities were corrected by multiplying by the square of the order number (h^2) for a powder pattern (unoriented samples) and a correction factor, $P(h)$, due to the geometry of the linear (one-dimensional) PSPC [33]. Hence, the structure factor, $F(h)$, equals $\sqrt{h^2 I(h) P(h)}$ $j(h)$, where $j(h)$ is the phase information for each order h. Electron density distributions, $\rho(x)$, were calculated by use of the formula:

$$\rho(x) \propto \Sigma \sqrt{h^2 I(h) P(h)}\, j(h) \cos(2\pi h x / d_l)$$

where d_l is a spacing. For a centrosymmetric $\rho(x)$ function, $j(h)$ must be either $+1$ or -1 for each order h. We calculated electron density distributions $\rho(x)$ of DPPC-MLV by using the SAXS data ($h_{max} = 4$), and $\rho(x)$ of POPC-MLV by using the SAXS data ($h_{max} = 3$).

2.4. Differential scanning carolimetry (DSC)

Differential scanning calorimetry (DSC) experiments were performed using a Rigaku DSC-8230B instrument. DPPC-MLV dispersions (1.4 wt.% lipid) were heated at a rate of 2.0°C/min. The main transition temperature and pre-transition temperature were determined as the onset of the endothermic transition extrapolated to the baseline. The details were described in our previous paper [3].

2.5. Measurement of solubility

Excess amounts of phosphorylcholine were mixed with various concentrations of DMF aqueous solution in order to make saturated solutions, and the unsolubilized powders were separated from the solutions by filtration and dried under vacuum. Solubilities of phosphorylcholine in these solution were determined by the weight of the unsolubilized powder. The solubilities determined by this method were overestimated, especially in the region of the low solubility. In this report, we did not use the Bartlett method to prevent a decomposition of DMF in high concentration of H_2SO_4 at high temperature for safety [35]. Therefore the values of the solubilities of phosphorylcholine in various concentrations of DMF had some uncertainty, although those in various concentrations of acetone had a high accuracy [28]. However, the result in this report is qualitatively correct.

3. Results

3.1. Dependence of solubility of phosphorylcholine in water on DMF concentration

We can get any information about the free energy of the interaction between the solvents, such as acetone and the hydrophilic segments of the PC (phosphatidylcholine) membrane surface, such as DPPC, by measuring solubilities of the phosphorylcholine molecule, that has the same molecular structure as the head-group of PC, in the mixture of the solvent and water [28]. We have investigated the dependence of solubility of phosphorylcholine on DMF concentration in a DMF–water mixture. Fig. 1 shows that the solubilities of the phosphorylcholine decreased with an increase in DMF concentration. This qualitative result indicates that DMF is a poor solvent for the hydrophilic segments of the PC membrane, and an interaction free energy, that is, a χ parameter (interaction energy parameter) of the hydrophilic segments of the PC membrane with solvent increases with an increase in DMF concentration.

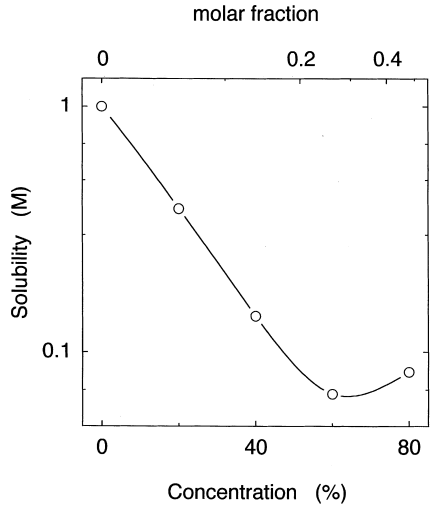

Fig. 1. Solubility of phosphorylcholine in various concentrations of DMF [% (v/v) or molar fraction] in a DMF–water mixture at 20°C. The solubility was measured by the method described in Section 2.

3.2. Structure and intermembrane distance of DPPC-MLV in the gel phase in a DMF–water mixture

DPPC-MLV at 20°C is well known to be in the gel ($L_{\beta'}$) phase [28,36]. We have investigated the dependence of spacing (lamellar repeat period) and intermembrane distance of DPPC-MLV on DMF concentrations by SAXS. As shown in Fig. 2, the spacing (d_l) of DPPC-MLV at 20°C gradually decreased from 6.5 (0% DMF) to 5.7 nm [80% (v/v) DMF] with an increase in DMF concentration.

We have determined electron density profiles of the DPPC-MLVs in various concentrations of DMF, in order to estimate their intermembrane distances. To get the electron density profiles by using the equation in Section 2.3, we determined phases, $j(h)$, as follows. As shown in Fig. 2, the spacing changed from 6.5 to 5.7 nm. Using the

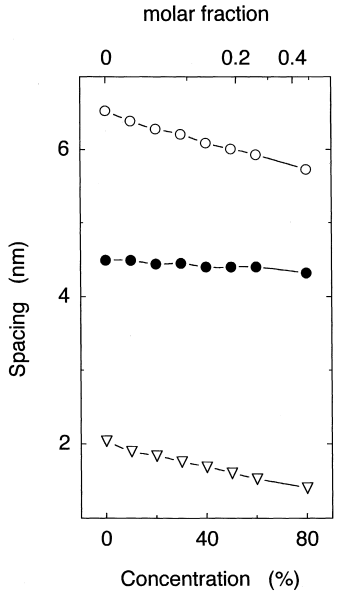

Fig. 2. The spacing (d_l) (○), the membrane thickness (d_m) (●), and the intermembrane distance (d_f) (▽) of DPPC-MLV in various concentrations of DMF [% (v/v) or molar fraction] in a DMF–water mixture at 20°C. The membrane thickness (d_m) was estimated to be d_{p-p}, which was determined by the electron density profiles. The intermembrane distance (d_f) was estimated to be ($d_l - d_{p-p}$) (nm). The details were described in the text.

shift of the spacings, we plotted a structural factor, $F(h)$, vs. reciprocal space coordinate, s ($s = h/d_l$) (Fig. 3) [28,37]. From this graph, we determined that sets of the phase $j(h)$ are $(-1, -1, +1, -1)$ for orders $h = 1-4$. This phase is the same as that of the $L_{\beta'}$ phase of DPPC-MLV [28,37]. Fig. 4a,b show electron density profiles of DPPC-MLV in 0% (v/v) and 80% (v/v) DMF, respectively. From the profiles, the distance between head-group peaks across the bilayer, d_{p-p}, at 0 and 80% (v/v) DMF were 4.5 and 4.3 nm, respectively. We estimated the membrane thickness to be d_{p-p}, and the fluid layer thickness (d_f), that is, intermembrane distance, to be $d_l - d_{p-p}$. This estimation of d_f is overestimated, because the fluid layer determined by this definition contains the head-group region of the phospholipid. From Fig. 4, the intermembrane distance (d_f) at 0 and 80% (v/v) DMF were 2.0 and 1.4 nm, respectively. Fig. 2 also shows that d_f decreased with an increase in DMF concentration (0–80%), although the d_{p-p} were almost the same.

Wide-angle reflections of DPPC-MLV in various concentrations of DMF [0–80% (v/v)] at 20°C were investigated with high accuracy by using the PSPC with the sample-to-detector distance of 250 mm (Fig. 5), which showed that

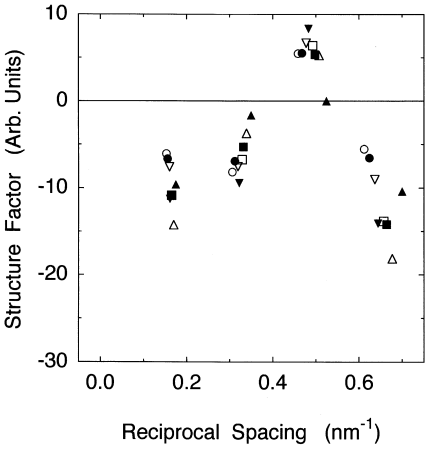

Fig. 3. Plots of structure factor vs. reciprocal space coordinate for SAXS data of DPPC-MLV at 20°C in various DMF concentration: (○) 0%; (●) 10%; (▽) 20%; (▼) 30%; (□) 40%; (■) 50%; (△) 60%; (▲) 80% (v/v) DMF.

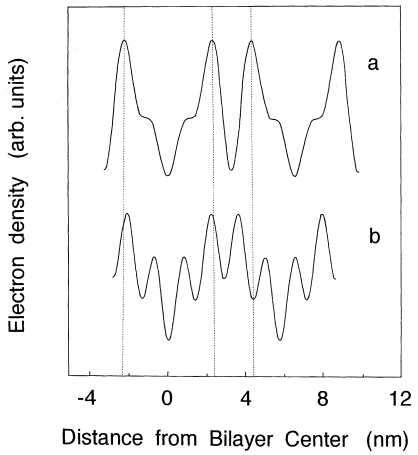

Fig. 4. Electron density profiles for DPPC-MLV in (a) 0%, (b) 80% (v/v) DMF at 20°C. Abscissa is a distance from the bilayer center (nm). For each profile, the geometric center of the bilayer is placed at the origin of the abscissa. The low density region in the center of the profile corresponds to the phospholipid hydrocarbon chains and the high density peaks on either side correspond to the lipid head-groups.

DPPC-MLVs from 0 to 80% (v/v) DMF were in the bilayer gel phase. They were almost the same in the low concentrations of DMF [$\leq 30\%$ (v/v)]; they consisted of a strong, sharp reflection at 0.424 nm and a diffuse reflection centered at 0.412 nm. The WAXS spacings depend on the distance of the alkyl chains in the membrane. The separation in the WAXS spacing occurs by means of inclination of alkyl chains, which is characteristic of the $L_{\beta'}$ phase [28,36]. Above 30% DMF, the WAXS spacing of the strong reflection decreased with an increase in DMF concentration. At 80% (v/v) DMF, the WAXS pattern of DPPC-MLV consisted of a strong, broad reflection at 0.416 nm and a weak, broad reflection at 0.424 nm.

3.3. Phase transition of DPPC-MLV in various concentrations of DMF

DSC heating curves of DPPC-MLV in the presence of DMF are shown in Fig. 6. There were two endothermic transition peaks in 0% DMF, which correspond to pre- and main transition. Main transition temperature (chain-melting transition temperature), T_m, and pre-transition temperature

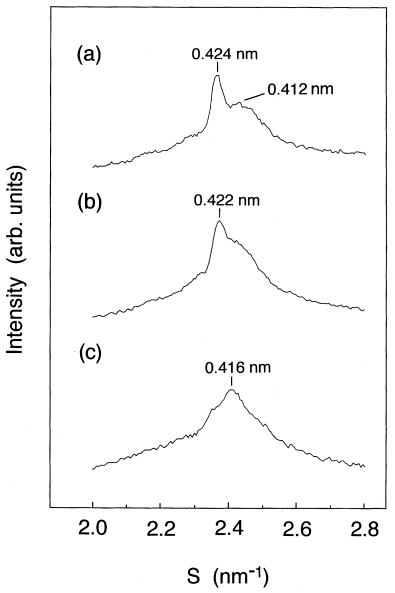

Fig. 5. Wide-angle X-ray diffraction patterns of DPPC-MLV at 20°C in various DMF concentration: (a) 0%; (b) 50%; (c) 80% (v/v) DMF.

from $L_{\beta'}$ to ripple phase ($P_{\beta'}$), T_p, were determined as the onsets of the endothermic transitions extrapolated to the baseline. T_m of DPPC-MLV increased with an increase in DMF concentration from 41.6 (0%) to 47.3°C (80% DMF) (Fig. 7). T_p of DPPC-MLV increased more rapidly with an increase in DMF concentration. As shown in Fig. 7, above 50% (v/v) DMF, there was no pre-transition. The enthalpy change of the main transition (ΔH) increased a little with an increase in DMF concentration below 40% (v/v) DMF; 8.7 kcal/mol at 0% DMF, and 9.5 kcal/mol at 30% DMF. Above 40% DMF, it was difficult to determine ΔH values reproducibly because of the precipitation of DPPC-MLV in the suspension.

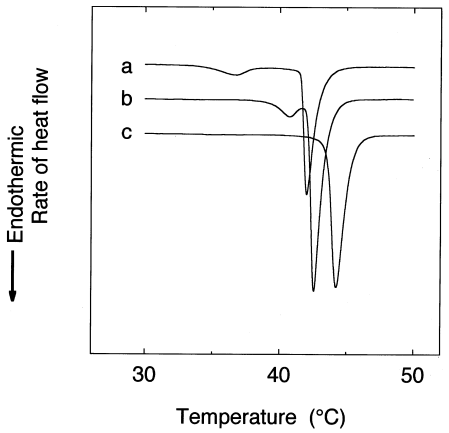

Fig. 6. Differential scanning calorimetry heating curves of DPPC-MLV in various DMF concentration. (a) 0%; (b) 40%; (c) 60% (v/v) DMF. Heating rate were 2.0°C/min.

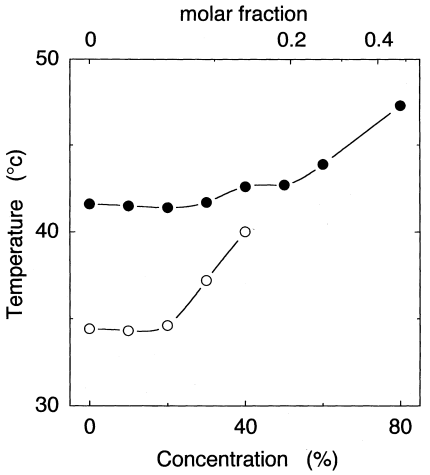

Fig. 7. Main transition temperature (●) and pre-transition temperature (○) of DPPC-MLV in various concentrations of DMF [% (v/v) or molar fraction]. Heating rate was 2.0 K/min. The transition temperatures were determined as the onset of the endothermic transition extrapolated to the baseline.

3.4. Structure and intermembrane distance of POPC-MLV in the liquid-crystalline phase in a DMF–water mixture

POPC-MLV in excess water at 20°C is well known to be in the liquid-crystalline (L_α) phase [36]. We have investigated a dependence of spacing and intermembrane distance of POPC-MLV on DMF concentrations by SAXS. As shown in Fig. 8, the spacing (d_l) of POPC-MLV at 20°C gradually decreased from 6.5 (0% DMF) to 4.5 nm [80% (v/v) DMF] with an increase in DMF concentration. Wide-angle reflections of POPC-MLV in various concentrations of DMF (0–80%) at 20°C were almost the same; they consisted of a diffuse broad band at approx. 0.44 nm, which is

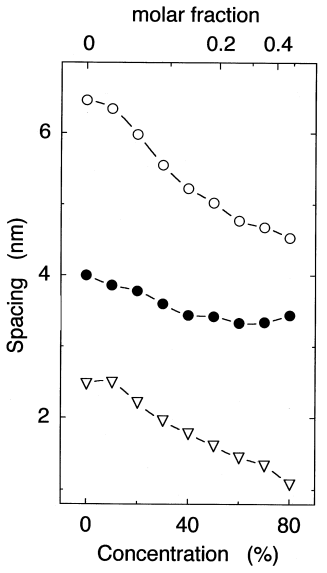

Fig. 8. The spacing (d_l) (○), the membrane thickness (d_m) (●), and the intermembrane distance (d_f) (▽) of POPC-MLV in various concentrations of DMF [% (v/v) or molar fraction] in a DMF–water mixture at 20°C. The membrane thickness (d_m) was estimated to be d_{p-p}, which was determined by the electron density profiles. The intermembrane distance (d_f) was estimated to be ($d_l - d_{p-p}$) (nm). The details were described in the text.

characteristic of L_α phase. These results show that the POPC-MLVs in various concentration of DMF (0–80%) were in the L_α phase.

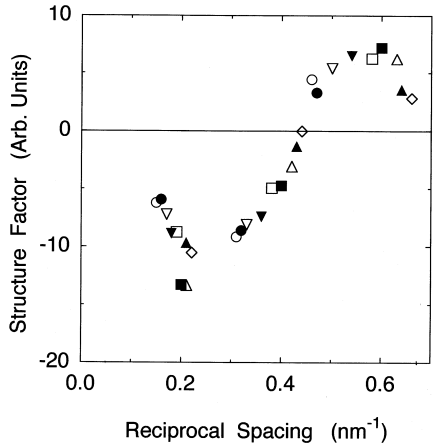

Fig. 9. Plots of the structure factor vs. the reciprocal space coordinate for SAXS data of POPC-MLV at 20°C in various DMF concentration: (○) 0%; (●) 10%; (▽) 20%; (▼) 30%; (□) 40%; (■) 50%; (△) 60%; (▲) 70%; (◇) 80% (v/v) DMF.

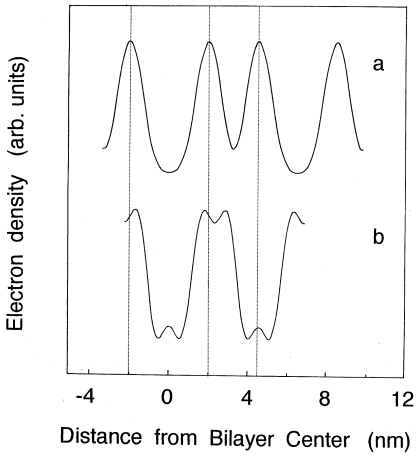

Fig. 10. Electron density profiles for POPC-MLV in (a) 0%, (b) 80% (v/v) DMF at 20°C. Abscissa is a distance from the bilayer center (nm). For each profile, the geometric center of the bilayer is placed at the origin of the abscissa.

We have determined electron density profiles of the POPC-MLVs in various concentration of DMF, in order to estimate their intermembrane distances. To get the electron density profiles, we determined phases, $j(h)$, by the same method described in Section 3.2. Using the shift of the spacings from 6.5 (0%) to 4.5 nm (80% DMF), we plotted a structural factor, $F(h)$, vs. a reciprocal space coordinate, s ($s = h/d_l$) (Fig. 9) [28,37]. From this graph, we determined that sets of the phase $j(h)$ are $(-1, -1, +1)$ for orders $h = 1$–3. This phase is the same as that of the L_α phase of POPC-MLV [36]. Fig. 10a,b show electron density profiles of POPC-MLV in 0 and 80% (v/v) DMF, respectively. From the profiles in Fig. 10, the fluid layer thickness (d_f) at 0 and 80% (v/v) DMF were 2.5 and 1.1 nm, respectively. Fig. 8 also shows that the fluid layer thickness (d_f) largely decreased with an increase in DMF concentration, although the d_{p-p} decreased a little from 4.0 (0%) to 3.4 nm (80%).

4. Discussion

4.1. Interaction free energy between solvents and the hydrophilic segments of the membrane surface

Phospholipid membranes and biomembranes can be treated as a two-dimensional semiflexible

polymer sheet (main chain) connected by the hydrophobic interaction and van der Waals interaction in the alkyl chains of the lipids, and also this polymer sheet has flexible side chains, i.e. head-groups of the phospholipids. The local out-of-plane motions of lipids, protrusion (amplitude of 0.2–0.3 nm [2,15,16]) make roughness of the membrane surface, and thermal fluctuations can excite pronounced bending undulation of the membrane [15,16,39,43]. Owing to these dynamic membrane roughness and flexibility of the head-groups of the phospholipids, the phospholipid membrane may be considered as a two-dimensional semiflexible polymer with side chains.

Recently, we have proposed that the interaction free energy of the segments of the membrane surface of biomembrane and phospholipid membranes with solvents, play an important role in structure and phase behaviors of these membranes [28–30]. In good solvents, where the interaction between the segments and the solvents is favorable, the segments expand to contact the solvents; on the other hand, in poor solvents, where their interaction is unfavorable, the segments shrink or associate with each other to prevent the contact with the solvents. As a measure of the interaction free energy of surface segments of the membrane with solvents, a χ parameter is introduced;

$$\chi = \Delta G / 2k_B T \quad (1)$$

where ΔG is a free energy increase associated with the contact of segments with solvent, or a free energy decrease associated with the contact between segments, k_B and T are Boltzmann constant and absolute temperature, respectively. In good solvents, χ is small; on the other hand, in poor solvents, χ is large. In the field of polymer science, this kind of χ parameter can describe well the thermodynamic properties of macromolecules in solvents [21–23]. In biomembranes, water is a good solvent for the hydrophilic segment of membrane surface, and thereby, the intermembrane distance of the MLV in water is large.

In our previous paper [28], we indicated that acetone was a poor solvent for phosphorylcholine, and thereby, it was a poor solvent for the hydrophilic segments for the surface of the PC (phosphatidylcholine) membranes, and also that the χ parameter of the hydrophilic segments of the surface of PC membranes with solvents increased with an increase in acetone concentration. The result of Fig. 1 indicates that DMF is another poor solvent for the phosphorylcholine, and thereby for the hydrophilic segments for the surface of the PC membranes, and also that the χ parameter of the hydrophilic segments of the surface of the PC membrane increases with an increase in DMF concentration.

4.2. Decrease of intermembrane distance of DPPC-MLV and POPC-MLV with increasing DMF concentration

Fig. 2 shows that the intermembrane distance, that is, the fluid layer thickness (d_f) of DPPC-MLV in the gel phase gradually decreased with increasing DMF concentration. Fig. 8 shows that the intermembrane distance of POPC-MLV in the $L\alpha$ phase decreased with an increase in DMF concentration. The decrement of the intermembrane distance of the PC-MLV in the $L\alpha$ phase was much larger than that in the gel phase.

In our previous paper [28], we estimated the intermembrane distance to be $[d_l - (d_{p-p} + 1.0)]$ (nm), because we assume that a head-group is, on average, oriented approximately parallel to the bilayer plane in the $L_{\beta'}$ phase, and thereby, the edge of the bilayer lies approx. 0.5 nm outward from the center of the high density peaks in the electron density profiles [7]. However, the conformation of the hydrophilic segment may change in various concentrations of solvents, and also in the L_α phase this assumption does not hold. Therefore in this paper, we estimated the intermembrane distance to be $(d_l - d_{p-p})$, which can eliminate the effect of conformational changes of the hydrophilic segment on the intermembrane distance.

The decrease in the intermembrane distance of MLV may be explained as follows. Intermembrane interactions of biomembranes are very important factors in stability and dynamic structures of vesicles of biomembranes. Among several

methods to investigate the intermembrane interactions, the approach to determine main factors controlling an equilibrium intermembrane distance in the phospholipid-MLV has been considered one of the best methods, and their various kinds of experimental and theoretical approaches have been done [1,5,38,39]. Most investigators have tackled this problem by considering the force balance between the bilayers; van der Waals attractive force balances repulsive forces between the bilayers [5,38,39]. The repulsive forces for neutral phospholipid membranes (net charge of the head-group of the phospholipid is zero) such as DPPC and POPC are due to undulation motion, peristaltic motion, protrusion, steric overlap of head-groups, and hydration force [38,39].

The van der Waals attractive force per unit area between two planar surfaces, P_v, can be calculated by;

$$P_v = -H/6\pi D^3 \tag{2}$$

where H is the non-retarded Hamaker constant and D is the separation of the two planar surfaces [39]. The Hamaker constant, H, for the interaction of phospholipid membranes can be expressed by the static dielectric constant and refractive indices of the membrane and fluid phase based on the Lifshitz theory [39] as follows;

$$H \approx 3kT/4(\varepsilon_l - \varepsilon_f/\varepsilon_l + \varepsilon_f)^2 + 3h\nu_e\left(n_l^2 - n_f^2\right)^2 /16\sqrt{2}\left(n_l^2 + n_f^2\right)^{3/2} \tag{3}$$

where $h\nu_e$ is the ionization energy of the bilayer (approx. 2×10^{-18} J), ε's are the static dielectric constants, and n's are the indices of refraction, where the subscripts l and f refer to the bilayer and fluid phases, respectively. The dielectric constant and refractive index of the phospholipid membranes are 2.0 and 1.45, respectively [40,41]. Dielectric constant of the fluid phase decreases with an increase in DMF concentration from 80.2 (pure water, 0% DMF) to 38.3 (100% DMF), and the refractive index of the fluid phase increases slightly with an increase in DMF concentration from 1.333 (pure water) to 1.432 (100% DMF). A calculation by Eq. (3) shows that Hamaker constant, H, decreases with an increase in DMF concentration, and when water is replaced with DMF, it decreases by 60%. This rough calculation suggests that the van der Waals attractive force between the membranes may decrease significantly with an increase in DMF concentration. Therefore the experimental results and this calculation suggest that the repulsive interactions between the membranes have to decrease largely with an increase in DMF concentration to induce the decrease in the intermembrane distance in the MLV.

As the concentration of the poor solvents such as DMF increases, the interaction free energy (or χ parameter) between the hydrophilic segments and solvents increases, which induce a shrinkage of the head-group region of the hydrophilic segments, consisting of the segments and solvents. The overlap of the head-group segments is considered to induce the repulsive force between the membranes [39]. Therefore the increase in the χ parameter may decrease the steric interaction of the head-groups, inducing a decrease in the repulsive interactions between the membranes. It may also induce a decrease in the interfacial area of the membrane with solvents, which may restrain the protrusion and the undulation of the membranes (see discussion below). Thereby, the repulsive interactions between the membranes may decrease with an increase in DMF concentration, which induce a decrease in intermembrane distance in the MLV to overcome the decrease in the van der Waals attractive force between the membranes.

The undulation motion of the membrane in L_α phase has been considered to play an important role in intermembrane interactions [15,16,42,43], which is much larger than that in the $L_{\beta'}$ phase, and thereby, the intermembrane distance of MLV in the L_α phase has been considered larger than that in the $L_{\beta'}$ phase [42]. The undulation motion of the membranes is related with the bending modulus (or the elastic curvature modulus) of the membrane, κ [15,39], and the repulsive undulation force per unit area, P_u, between the membranes can be expressed as;

$$P_u \approx (k_B T)^2 / 2\kappa D^3 \quad (4)$$

where D is the intermembrane distance, and k_B is the Boltzmann constant. Eq. (4) shows that the undulation force decreases with an increase in κ. The decrements in the intermembrane distance of the POPC-MLV in the L_α phase induced by DMF (Fig. 8) were larger than those of DPPC-MLV in the gel phase (Fig. 2). This result can be explained as follows. In equilibrium, three kinds of lateral pressures in the membrane have to balance as follows [39]:

$$\Pi_{\text{head}} + \Pi_{\text{chain}} = \gamma \quad (5)$$

where Π_{head} is the head-group pressure due to the repulsive interaction between the head-groups of the phospholipid such as a steric interaction and electrostatic interaction, Π_{chain} is the repulsive chain pressure, and γ is the attractive interfacial pressure due to the hydrophobic interaction between the alkyl chains and water at the membrane surface. As DMF concentration in the aqueous phase increases, that is, the interaction free energy (or χ parameter) increases, the amount of solvents in the head-group regions decreases, and thereby, the more shrinkage of the head-group region of the phospholipid membrane may occur. This shrinkage may decrease the steric interaction between the head-groups, and thereby, decrease Π_{head}. We can assume that γ is constant in the presence of various concentrations of DMF, because the DMF molecule is so large that it cannot enter into the head-group region (see Section 4.3). Therefore a lateral compression pressure of the membrane, $\gamma - \Pi_{\text{head}}$, increases with an increase in DMF concentration. The results of WAXS of DPPC-MLV in the presence of various concentration of DMF (Fig. 5) shows that the distance of the alkyl chains of DPPC decreased with an increase in DMF concentration, which supports the above hypothesis. This lateral compression of the membrane also may be one of the main reasons of the increase in main transition and pre-transition of DPPC-MLV with an increase in DMF concentration (Fig. 7), as discussed in the increase in main transition temperature of DPPC-MLV induced by the osmotic stress [3]. This lateral compression of the alkyl chains and also the shrinkage of the head-group regions to prevent the contact between the hydrophilic segments with solvents, may decrease the surface area of the membranes, and increase the bending rigidity of the membranes. Hence, the increase in the interaction free energy (or χ parameter) induced by the presence of DMF may increase the bending modulus, κ, of the membrane, inducing the decrease in the undulation force of the membrane according to Eq. (4). This may be one of the main reasons of a larger decrease in the intermembrane distance of the MLV in the L_α phase.

When we consider the phospholipid membranes as elastic thin sheets, the bending modulus κ can be related with the elastic modulus of the isothermal compression, K_A, as follows [44]:

$$\kappa = K_A \delta^2 / 2 \quad (6)$$

where δ is the distance between the polar–apolar interfaces in the membrane, or the membrane thickness. Fig. 8 shows that d_{p-p} of POPC-MLV decreased a little with an increase in DMF concentration, which suggests apparently that δ decrease with an increase in DMF concentration. If we consider that K_A would be constant with increasing DMF, the above result would yield a decrease in bending modulus κ, which contradicts our hypothesis described in the preceding paragraph. However, at present, we have at least two unresolved problems: a relationship between δ and d_{p-p}; and also a dependence of K_A on DMF concentration. We have determined d_{p-p} as the distance between head-group peaks across the bilayer from the electron density profiles, and thereby, $d_{p-p} = \delta + \alpha d_h$, where d_h is the thickness of the head-group region and α is a constant. There is a possibility that the orientation of the head-group of POPC-MLV may become more parallel to the membrane surface, and thereby, d_h may decrease with an increase in DMF concentration. In this case, d_{p-p} may decrease without a change of δ with an increase in DMF concentration. Alternatively, the elastic modulus of the isothermal compression, K_A, would increase with increasing DMF concentration, and thereby, a

large increase in K_A might increase κ irrespective of the small decrease in δ according to Eq. (5). Further investigations on effects of χ parameter, that is, DMF concentration, on the undulation motion are necessary by a direct measurement of the bending modulus κ and the elastic modulus of the isothermal compression K_A of the membranes in the various concentration of DMF, and by an analysis of peak shapes of X-ray scattering at high instrumental resolution [45].

In order to calculate van der Waals forces of phospholipid membranes, LeNeveu et al. [46] assumed that the MLV of the phospholipid consisted of three different continuous media: the hydrocarbon layer of the membrane; hydrated polar groups layer; and aqueous layers between the membranes; and intended to include the effect of the polar groups layers on van der Waals forces between the membranes by using the Lifshitz theory. However, as they mentioned, their estimation of the dielectric permeabilities of the polar group layer were not reliable, and it is difficult to consider the hydrated polar groups layer as the continuous media. On the other hand, in our χ parameter theory, we consider the polar layer microscopically, not the continuous media, and treated it as a mixture of surface segments and solvents, and thereby, the interaction between the polar segments in solvents is expressed by the interaction free energy of surface segments of the membrane with solvents (χ parameter), not by the Lifshitz theory. The χ parameter is mainly determined by the van der Waals interaction between the surface segments, between solvents, and between the surface segments and solvents [22], and therefore, it is a useful parameter of the interaction between discontinuous media such as polymers in solvents.

McIntosh et al. [41] showed that egg PC could form MLVs in neat (100%) formamide or in neat 1,3-propanediol, and repulsive forces per unit area between the bilayers in these solvents could be expressed as follows:

$$P = P_0 \exp(-D/\lambda) \quad (7)$$

where λ is the decay length of the repulsive force, P_0 is the magnitude of the repulsive force, and D is the intermembrane distance. The decay length λ for egg PC bilayers in water, formamide, and 1,3-propanediol was found to be 1.7, 2.4, and 2.6 Å. These results clearly showed that the exponentially repulsive force between the membranes is not unique to water or so-called hydration force. They considered that the decay length depended on the packing of the solvent molecules, and the magnitude of the solvation force depends on the square of the dipole potential of the membrane. On the other hand, by using these data, Israelachvili and Wennerström argued that the interfacial energy of the hydrocarbon–solvent interface decreased in the presence of these non-aqueous solvents, and thereby, the protrusion force of the membrane increased [2]. However, DMF is a larger molecule than formamide or 1,3-propanediol, and thereby, it can not penetrate into the head-group region. This hypothesis can be proved by the fact that DMF can not induce the interdigitated gel phase (see Section 4.3), and on the other hand, formamide and 1,3-propanediol can induce the interdigitated gel phase in DPPC-MLV at high concentrations (Furuike et al., manuscript in preparation). Therefore we can assume that the interfacial energy of the hydrocarbon–solvent interface may not change largely in the presence of DMF, and thereby, the protrusion force of the membrane may not increase.

4.3. DMF does not induce an interdigitated gel phase in DPPC-MLV

In the presence of several alcohols such as ethanol and glycerol, DPPC-MLV can form the interdigitated gel ($L_\beta I$) phase [47,48]. Recently, we have found that several water-soluble organic solvents other than alcohols, such as acetone, acetonitrile, propionaldehyde, and tetrahydrofurane, also induce $L_\beta I$ phases in DPPC-MLV at their low concentrations [29]. In the previous paper [29], we proposed a new hypothesis for a mechanism of the induction of the $L_\beta I$ phase in PC-MLV that this $L_\beta I$ phase is induced by water-soluble organic solvent molecules which have a high solubility for alkane and also can penetrate into the interfacial regions between the

segments of the terminal alkyl chain and water in the $L_{\beta}I$ phase or (and) into the interfacial region between the head-groups in $L_{\beta'}$ phase. The results in this report clearly showed that a water-soluble organic solvent — DMF — did not induce an $L_{\beta}I$ phase in DPPC-MLV, although DMF has a relatively high solubility for alkane. A DMF molecule has a large hydrophilic part, and thereby, it is difficult to penetrate into the interfacial regions of the DPPC membrane in gel phase. This may be one of the main reasons why DMF can not induce the $L_{\beta}I$ phase in DPPC-MLV. On the other hand, formamide has a similar chemical property as DMF, but it can induce the interdigitated gel phase in DPPC-MLV at high concentrations, because it is much smaller molecule than that DMF, and thereby, it can penetrate into the interfacial regions (Furuike et al., manuscript in preparation). Therefore these results clearly support our hypothesis [29] for a mechanism of the induction of the $L_{\beta}I$ phase in phospholipid membranes.

Acknowledgements

This work was supported partly by a Grant-in Aid for General Scientific Research C (Grant 07808073) from the Ministry of Education, Science, and Culture, Japan (to M.Y.).

References

[1] J.N. Israelachvili, H. Wennerstöm, Nature 379 (1996) 219.
[2] J.N. Israelachvili, H. Wennerstöm, J. Phys. Chem. 96 (1992) 520.
[3] M. Yamazaki, M. Ohshika, N. Kashiwagi, T. Asano, Biophys. Chem. 43 (1992) 29.
[4] M. Yamazaki, S. Ohnishi, T. Ito, Biochemistry 28 (1989) 3710.
[5] R.P. Rand, V.A. Parsegian, Biochim. Biophys. Acta. 988 (1989) 351.
[6] A.S. Ulrich, A. Watts, Biophys. J. 66 (1994) 1441.
[7] S.A. Simons, E.A. Disalvo, K. Gawrish, et al., Biophys. J. 66 (1994) 1943.
[8] M. Yamazaki, N. Kashiwagi, M. Miyazu, T. Asano, Biochim. Biophys. Acta 1109 (1992) 43.
[9] M. Yamazaki, M. Miyazu, T. Asano, Biochim. Biophys. Acta 1106 (1992) 94.
[10] M. Yamazaki, M. Miyazu, T. Asano, A. Yuba, N. Kume, Biophys. J. 66 (1994) 729.
[11] H. Takahashi, S. Matsuoka, S. Kato, K. Ohki, I. Hatta, Biochim. Biophys. Acta. 1069 (1991) 229.
[12] U. Vierl, L. Löbbecke, N. Nagel, G. Cevc, Biophys. J. 67 (1994) 1067.
[13] S. Chiruvolu, H. Warriner, E. Naranjo, et al., Science 266 (1994) 1222.
[14] E.S. Rowe, J.M. Campion, Biophys. J. 67 (1994) 1888.
[15] E. Sackmann, Science 271 (1996) 43.
[16] R. Lipowsky, Nature 349 (1991) 475.
[17] S.-J. Marrink, M. Berkowitz, H.J.C. Berendsen, Langmuir 9 (1993) 3122.
[18] G. Cevc, M. Hauser, A.A. Kornyshev, Langmuir, 11 (1995) 3103;3111.
[19] K. Tu, D.J. Tobias, K. Blasie, M.L. Kiein, Biophys. J. 70 (1996) 595.
[20] S.-W. Chiu, M. Clark, V. Balaji, S. Subramaniam, H.L. Scott, E. Jakobssson, Biophys. J. 69 (1996) 1230.
[21] P.J. Flory, Principles of Polymer Chemistry. Cornell University Press, Ithaca, 1953.
[22] P.-G. de Gennes, Scaling Concepts in Polymer Physics. Cornell University Press, Ithaca, 1979.
[23] M. Doi, Introduction to Polymer Physics, Oxford University Press, 1995.
[24] T. Tanaka, Phys. Rev. Lett. 40 (1978) 820.
[25] T. Tanaka, D. Fillmore, S.-T. Sun, I. Nishio, G. Swislow, A. Stah, Phys. Rev. Lett. 45 (1980) 1636.
[26] Y. Li, T. Tanaka, Ann. Rev. Mater. Sci. 22 (1992) 243.
[27] M. Annaka, T. Tanaka, Nature 355 (1992) 430.
[28] K. Kinoshita, T. Asano, M. Yamazaki, Chem. Phys. Lipids 85 (1997) 53.
[29] K. Kinoshita, M. Yamazaki, Biochim. Biophys. Acta 1284 (1996) 233.
[30] K. Kinoshita, M. Yamazaki, Biochim. Biophys. Acta 1330 (1997) 199.
[31] M. Yamazaki, K. Kinoshita, A. Asano, Abstract of Annual Meeting of Physical Society Japan, Kanazawa, 3 (1996) 749.
[32] K. Kinoshita, S. Furuike, M. Yamazaki, Biophys. Jpn. 36/S (1996) 113.
[33] O. Glatter, O. Kratky (Eds.), Small Angle X-ray Scattering, Academic Press, 1982.
[34] P.H. Geil, Polymer Single Crystals, Interscience Publishers, 1963.
[35] G.R. Barlett, J. Biol. Chem. 234 (1959) 466.
[36] A. Tardieu, V. Luzzati, J. Mol. Biol. 75 (1973) 711.
[37] J. Torbet, M.H.F. Wilkins, J. Theor. Biol. 62 (1976) 447.
[38] T.J. McIntosh, S.A. Simon, Annu. Rev. Biophys. Biomol. Struct. 23 (1994) 27.
[39] J.N. Israelachvili, Intermolecular and Surface Forces, 2nd ed., Academic Press, 1992.
[40] R.J. Cherry, D. Chapman, J. Mol. Biol. 30 (1969) 551.
[41] T.J. McIntosh, A.D. Magid, S.A. Simons, Biochemistry 28 (1989) 7904.
[42] T.J. McIntosh, S. Advani, R.E. Burton, D.V. Zhelev, D. Needham, S.A. Simons, Biochemistry 34 (1995) 8520.

[43] W. Helfrich, Z. Naturforsch. 33a (1978) 305.
[44] G. Cevc, D. Marsh, Phospholipid Bilayers, John Wiley and Sons, 1987.
[45] J.F. Nagle, R. Zhang, S.-T. Nagle, W. Sun, H.I. Petrache, R.M. Suter, Biophys. J. 70 (1996) 1419.
[46] D.M. LeNeveu, R.P. Rand, V.A. Parsegian, D. Gingell, Biophys. J. 18 (1977) 209.
[47] S.A. Simons, T.J. McIntosh, Biochim. Biophys. Acta 773 (1984) 169.
[48] R.V. McDaniel, T.J. McIntosh, S.A. Simon, Biochim. Biophys. Acta 731 (1983) 97.